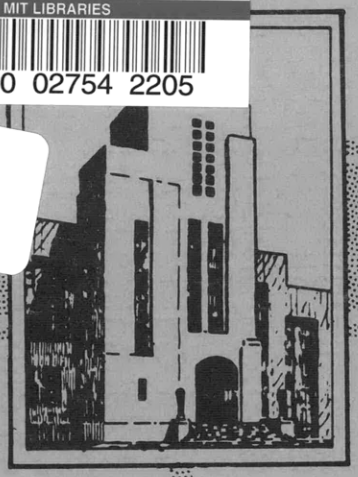

DEPARTMENT OF THE NAVY

DAVID TAYLOR MODEL BASIN

HYDROMECHANICS

AERODYNAMICS

STRUCTURAL MECHANICS

APPLIED MATHEMATICS

THE EFFECTS OF SCALE AND TOWING SYSTEM ON WAVE TESTS OF SMALL SHIP MODELS

by

Howard R. Reiss

HYDROMECHANICS LABORATORY

RESEARCH AND DEVELOPMENT REPORT

May 1961

Report 1039

THE EFFECTS OF SCALE AND TOWING SYSTEM ON WAVE TESTS OF SMALL SHIP MODELS

by

Howard R. Reiss

May 1961 Report 1039

TABLE OF CONTENTS

	Page
ABSTRACT	1
INTRODUCTION	1
TEST EQUIPMENT	2
GRAVITY DYNAMOMETER	2
SPEED MEASUREMENT	2
WAVEMAKER	3
WAVE MEASUREMENT	3
MOTIONS MEASUREMENT	4
TEST PROCEDURE	4
MODEL BALLASTING	4
DYNAMOMETER TARE	5
TOW WEIGHTS REQUIRED	5
CAMERA ALIGNMENT	6
RUNNING OF TESTS	6
TEST DATA	7
SPEED	7
WAVE SIZE	7
MODEL MOTIONS	8
Heave	8
Pitch	9
Phase Displacement	10
DISCUSSION OF RESULTS	11
GENERAL FEATURES	11
POSSIBLE CAUSE FOR DISCREPANCIES	11
Reynolds Number	11
Wave Reflection from Walls	12
Towing System Dynamics	13
CONCLUDING REMARKS	18
APPENDIX A - MEASUREMENT OF HEAVE	20
APPENDIX B - MEASUREMENT OF PHASE DISPLACEMENT	22
REFERENCES	24

LIST OF FIGURES

Page

Figure 1 - 5-Foot SAN FRANCISCO Model..... 25

Figure 2 - Sample Motions Record for Model 3572-8 in Wave of $\lambda/L = 1.25$ and $\lambda/H = 60$ for a Thrust Corresponding to 14-knot Still-Water Speed..... 26

Figure 3 - Sample Motions Record for Model 3572-8 in Waves of $\lambda/H = 60$ for a Thrust Corresponding to 10-knot Still-Water Speed..... 26

Figure 4 - Speed Reduction in Waves for Thrust Corresponding to 14-knot Still-Water Speed..... 27

Figure 5 - Speed Reduction in Waves for Thrust Corresponding to 10-knot Still-Water Speed..... 27

Figure 6 - Speed Reduction in Wave for $\lambda/H = 60$..... 28

Figure 7 - Ship Motions in Waves of $\lambda/H = 60$ for a Thrust Corresponding to 14-knot Still-Water Speed..... 29

Figure 8 - Ship Motions in Waves of $\lambda/H = 40$ for a Thrust Corresponding to 14-knot Still-Water Speed..... 30

Figure 9 - Ship Motions in Waves of $\lambda/H = 60$ for a Thrust Corresponding to 10-knot Still-Water Speed..... 31

Figure 10 - Ship Motions in Waves of $\lambda/H = 60$ for a Thrust Corresponding to 18-knot Still-Water Speed..... 32

Figure 11 - Example of Small Amplitude Motions Record. Model 3572-8 in Waves of $\lambda/L = 0.5$ and $\lambda/H = 60$ for a Thrust Corresponding to 10-knot Still-Water Speed..... 33

Figure 12 - Fluctuations in Pitch Angle, Model 3572-8..... 34

LIST OF TABLES

Page

Table 1 – Data for Model 3572-5A, V_s = 14 Knots, $\frac{\lambda}{H}$ = 60 35

Table 2 – Data for Model 3572-5A, V_s = 14 Knots, $\frac{\lambda}{H}$ = 40 35

Table 3 – Data for Model 3572-5A, V_s = 10 Knots, $\frac{\lambda}{H}$ = 60 36

Table 4 – Data for Model 3572-5A, V_s = 18 Knots, $\frac{\lambda}{H}$ = 60 36

Table 5 – Data for Model 3572-8, V_s = 14 Knots, $\frac{\lambda}{H}$ = 60 37

Table 6 – Data for Model 3572-8, V_s = 14 Knots, $\frac{\lambda}{H}$ = 40 37

Table 7 – Data for Model 3572-8, V_s = 10 Knots, $\frac{\lambda}{H}$ = 60 38

Table 8 – V_{min} for Model 3572-8 38

Table 9 – Natural Frequencies of Dynamometer 39

Table 10 – Maximum Fluctuation in Pitch Angle between Consecutive Cycles, Model 3572-8 39

NOTATION

a	Heave amplitude
c	Wave celerity
g	Gravitational acceleration
H	Wave height
h	Wave amplitude
L	Model length
ℓ	Height of midship's light above center of gravity of model
t	Time
v	Model speed
v_{min}	Minumum speed for which no interference from wall reflections occurs
V_s	Speed in still water of full-scale ship
v_s	Model speed in still water corresponding to V_s
W	Basin width
x, y, z	Coordinates
α	Phase displacement between pitch and heave
δ, ϵ	Angles
$\theta = \pi H/\lambda$	Maximum wave slope
Θ	Pitch amplitude
λ	Wave length
ν_e	Frequency of encounter with waves $\nu_e = \frac{1}{\lambda}\left[\sqrt{\frac{g\lambda}{2\pi}} + v\right]$
ν_n	Natural frequency of dynamometer
τ	Wavemaker period
ϕ	Pitch angle
ω	Circular frequency

ABSTRACT

To investigate experimentally the effect of scale on the motions of ship models in waves, two different scale models of the motor ship SAN FRANCISCO were tested. Although within the limits of the investigation there were no differences in the behavior of the models that could be ascribed to the effect of scale, several very noticeable effects were found that resulted from the dynamics of the towing system employed.

INTRODUCTION

The recent greatly increased interest in the seaworthiness of ships has focused attention upon the difficulties involved in an experimental study of the problem. Full-scale seaworthiness testing is not only extremely costly, but it also involves special problems of measurement and additional difficulties associated with lack of control over test conditions. For these reasons, much instrumentation has been developed and many test facilities have been devoted to the seaworthiness testing of reduced-scale models of ships. In particular, the use of very small models (on the order of 5-ft long) affords the considerable economics associated with small basins and wavemakers, small models, and relatively low manpower requirements. However, because seaworthiness is still incompletely understood, it is not known how faithfully a simple Froude scaling of model results to full-scale results represents the behavior of a ship in waves. Any shortcomings in the scaling will be magnified as smaller and smaller models are used. Thus it is essential to determine whether or not data from small models scale up properly before the conveniences offered by small models can be utilized.

In this investigation, two different sized models of the German motorship SAN FRANCISCO were tested at corresponding speed and wave conditions. Both models are small enough to be tested in the 140-ft

model basin at the David Taylor Model Basin. Since the same basin, wavemaker, and instrumentation could be used for both models, the number of possible explanations for any discrepancies between the two sets of results could be held to a minimum. However, because the displacement of the larger model was only about four times that of the smaller model, the maximum amplification of any scale effects could not be realized.

A series of tests was run in head seas at several wave lengths, wave heights, and tow forces; the speed, heave amplitude, pitch amplitude, and phase displacement between heave and pitch were measured. The data were analyzed and the results are examined in the light of the effects which are known not to scale.

TEST EQUIPMENT

GRAVITY DYNAMOMETER

The gravity dynamometer installed as permanent equipment in the 140-ft basin was used as the towing system. The geometry of the system and the dynamics of its motion are described in Reference 1.*

SPEED MEASUREMENT

Since in one revolution of the drive pulley of the dynamometer the model advances a distance equal to the circumference of the drive pulley, the average speed of the model during a period of revolution of the pulley can be determined by measuring this period and dividing it into the pulley circumference. The period measurement is accomplished by having the motion of the drive pulley interrupt a photocell-observed beam of light. The period is displayed digitally by an electronic interval timer. The

---

*References are listed on page 24

options are presented of either extending the period measurement over some selected number of cycles, or of alternately timing a single cycle and then displaying the result during the succeeding cycle.

A second light source and photocell system is used in conjunction with 40 equally spaced apertures in the drive pulley within the path of a light beam to provide an indication of the uniformity of the angular velocity of the pulley. The intervals between the pulses from the photocell are converted into a graphical record of velocity as a function of time. This system, termed a "speed deviation recorder," is used only in a qualitative fashion.

WAVEMAKER

The wavemaker installed in the 140-ft basin is a pneumatic type. Wave length control is achieved by setting the frequency of the air values with the aid of an electronic interval timer to find the period of rotation of the value drive. The wave height is set by adjusting the speed of the centrifugal blower which supplies the air to the wavemaker.

WAVE MEASUREMENT

The wave length is presumed to be uniquely established by the period of the wavemaker values. The

$$\lambda = \frac{g}{2\pi} \tau^2$$

between the wave length λ and the wavemaker period τ is sufficiently accurate for the present purposes.

The wave height is measured by a capacitance-type wave-height recorder described in detail in Reference 2.

MOTIONS MEASUREMENT

Measurements of the motions of the model as it is towed through waves were obtained from a photographic record of the progress of two small light sources fastened to the model. The lights, a type called "wheat lamps," are contained within thin brass tubes which support the lights at some distance above the deck of the model; see Figure 1. The tubes are provided with small holes to permit the lights to shine through as essentially point sources. The lights are elevated a sufficient distance above the deck to permit the camera to view them above the basin walls regardless of the model motion, without having to aim the camera downward over the basin wall. One light is located in the same transverse plane as the center of gravity of the model; the second light is located near the stern of the model. The after light is higher than the light at midships to keep the traces separate on the photographs. To record the motions of the lights during a run, the basin lights are extinguished and the camera shutter is kept open as the model progresses past the field of the camera.

Figures 2 and 3 are examples of the type of motions records obtained.

TEST PROCEDURE

MODEL BALLASTING

The models used were two of a series of models of SAN FRANCISCO whose dimensions are tabulated in Reference 3. The smaller model is 5 ft long. It is denoted as Model 3572-5A, and corresponds to Model 3572-5 in Reference 3. The larger model is 7.8 ft long, designated as Model 3572-8, and corresponds to Model 3572-4 in Reference 3. This 7.8-ft model is the largest which can be towed in the 140-ft basin without making resistance corrections because of the finite width (10 ft) of the basin.[4]

Model 3572-5A was ballasted to the appropriate displacement of 45.74 lb and trimmed to the waterline indicated in Reference 3. It was then arbitrarily assigned a radius of gyration in pitch of 1 ft and a vertical location of the center of gravity 0.78 in. below the waterline (2.63 in. above the keel). Model 3572-8 was ballasted to a corresponding displacement, radius of gyration in pitch, and center of gravity location. The methods given in Reference 5 were employed to achieve these results.

DYNAMOMETER TARE

The models were towed through waves by tow weights that were appropriate to achieve certain speeds of advance in still water. If the models and the basin water were kept scrupulously clean, the tow weight required for a given speed could vary only if the tare were to change. Hence a complete determination of the dynamometer tare as a function of speed was made at the beginning of the investigation, by the small corrections procedure described in Reference 6. Each morning a single point on the tare curve was checked at a speed typical of the runs to be conducted that day.

TOW WEIGHTS REQUIRED

It was desirable to introduce turbulence stimulation on the models. Two sand strips, one at the bow and another several inches aft of the first strip, were applied to both models.

The required tow weights and accelerating weights were found to tow Model 3572-5A at uniform speeds in still water which correspond to speeds of 10, 14, and 18 knots for the full-scale vessel. Model 3572-8 was towed only at speeds corresponding to 10 and 14 knots, and the required tow weights and accelerating weights were established.

By the use of the tow weights employed for the still-water speeds,

just mentioned, the proper accelerations to provide steady-state conditions in the test section of the basin were determined for each of the models at all wave conditions to be investigated. At 14 knots, wave heights equal to 1/60 and 1/40 of the wave length (or steepness ratios of 60 and 40) were used, and a steepness ratio of 60 was used for the 10-knot and 18-knot runs of the smaller model. In every case, wave lengths of 1/2, 3/4, 1, 1¼, and 1½ times ship length were investigated.

CAMERA ALIGNMENT

A camera which could accommodate a plate holder for 8- by 10-in. photographic plates was located to obtain a view of about 16 ft along the center plane of the basin in the center portion of the test section. The lens and plate holder were aligned with the vertical plane by means of a level on the camera. To set the camera's focal plane parallel to the plane of motion of the model (center plane of the basin), the basin was darkened and the model towed to one end of the field of vision of the camera. With a pair of dividers, the distance between the two lights on the model was measured on the camera's ground glass. The model was then towed to the other end of the camera's field of vision, and the distance between the model lights as they appeared on the ground glass was compared with the setting of the dividers. The camera was rotated to a position where the spacing of the lights on the model as imaged on the ground glass was independent of the location of the model. The camera alignment was checked regularly.

To reduce distortion during processing, all photographic data were recorded on glass plates.

RUNNING OF TESTS

With the basin lights extinguished, the model was towed to one end of the field of vision of the camera, and an exposure was made. Another

exposure on the same plate was made with the model at the other end of the camera's range. The model was then towed to its starting position and the basin water given time to calm. Then with the predetermined tow weights, acceleration, and wavemaker settings, the test was run while the camera shutter was left open to record the continuous motion of the model lights on the same plate which had been given the two previous static exposures. The wave height and model speed were recorded for each run. Every experimental condition was run twice.

TEST DATA

SPEED

The observed model speeds are listed in Tables 1 through 7. Speed reduction curves are shown in Figure 4 for 14-knot still-water speed, and in Figure 5 for 10-knot still-water speed. In Figure 6 are compiled the results for a wave steepness ratio of 60. Figures 4 through 6 show the measured speed averaged for the two runs at each condition and nondimensionalized with respect to V_s, the still-water speed. The wave lengths λ are nondimensionalized with respect to the model length L. Although the curves shown in Figures 4 through 6 are labeled with the nominal wave steepness ratios, no correction has been made for the fact that the actual wave heights deviated in general from the nominal values.

WAVE SIZE

Fluctuations in the period of the wavemaker values were usually limited to about 0.002 sec, which would thus produce an error in the wave length of about the same order of magnitude as the finite depth effect on the amplitude effect. These effects are small and are neglected.

Wave height measurements are accurate within 2 percent for heights of 1 in. or greater. Some fluctuations in wave height occurred during the run in many of the tests. The wave height was read from a portion of the wave record obtained about the time the model reached the location of the wave height probe. The probe was located near the end of the test section. The measured wave heights are listed in Tables 1 through 7. Nominal values for the wave heights are used in the graphical presentation of the data.

MODEL MOTIONS

Heave

The amplitude of heave was obtained by measuring the amplitude of the trace described by the light located in the same transverse plane as the center of gravity of the model. Because this light is raised above the center of gravity of the model, there exists a possibility that the amplitude of the trace may be affected by the pitching of the model. This possibility is examined in Appendix A, and the effect of pitch is found to be negligible.

The amplitudes of the traces were measured on a Bausch and Lomb comparator. The horizontal datum on the photographic plate is established by the static exposures that show the model lights at each end of the plate. The scale of the photograph can be determined by comparing the known distance between the two lights on the model with the distance as measured on the plate. A 50 X magnification was used in measuring the heave amplitude on the comparator. A combination of dial gage and micrometer permitted measurement of the amplitude of the trace to be made in increments of 0.0001 in. The arrangement of the comparator is such that this measurement is independent of the optics of the instrument and also independent of any backlash in the feed mechanism for the cross-slide. Because of the grain size and the thickness of the trace on the photograph, a measurement of the double amplitude of the trace could not be accomplished within 0.0001 in. but was probably closer to an uncertainty of about

0.0003 in. The horizontal ordinates at which the maxima and minima occurred were noted.

Heave measurements given by the average of the cycles shown on the plates are tabulated in Tables 1 through 7, and the average of the two runs at each condition is shown graphically and nondimensionalized in Figures 7 through 10. If the wave height is denoted by H, then the nondimensionalized amplitude of heave a is 2a/H. With h = H/2, 2a/H = a/h.

Pitch

To measure pitch on the comparator a 20 X magnification was used in conjunction with the protractor screen. The protractor screen for the comparator is a circular ground-glass screen, marked with horizontal and vertical reference lines, which can be rotated simply by turning a knob. The rotation of the screen is measured by a vernier protractor, which can be read in minutes of arc.

The plate was fastened to the carriage of the comparator as it was for the heave measurement; i.e., with the horizontal datum on the plate aligned with the direction of feed of the carriage. The distance between the two model lights as projected on the screen is laid off along the horizontal reference line on the screen, centered with respect to the screen center. The distance between the lights on the model was chosen so that it would be slightly less than the diameter of the screen when projected at 20 X magnification. By proper adjustment of the transverse and longitudinal feeds on the carriage and rotation of the screen, one end of the marked distance on the screen can be made to coincide with one trace. The other end of the marked distance is simultaneously made to lie on the other trace so that the two intersections mark points on the traces which were exposed simultaneously. Then the plate is fed longitudinally until a maximum or minimum of the screen rotation is reached. When a maximum or minimum of the pitching angle is found, the angle is recorded and the intersection of the lower trace (the trace from the midship's light) with the indicated distance on the screen is marked on the plate. This marked intersection is then moved to the vertical

centerline of the screen and its horizontal ordinate recorded.

The average pitch amplitudes, θ, are listed in Tables 1 through 7, and the averages of the two runs at each condition are plotted in Figures 7 through 10 as multiples of the maximum wave slope, $\theta = \pi H/\lambda$.

The only error in measuring the pitch angles is the error involved in fitting the inter-lights distance between the traces. This can be done within about 2 or 3 min, which is somewhat less than the normal fluctuation in pitch amplitude from cycle to cycle.

Phase Displacement

The phase displacement between pitch and heave is arrived at from information recorded during the measurement of the pitch and heave amplitudes. Because the midship's light is elevated above the center of gravity, the horizontal location of the midship's light at the time of an extremum in pitch or heave is not the location of the center of gravity of the model at that time. Further, the amount by which the horizontal location of the midship's light deviates from the horizontal location of the center of gravity is in general different at the time of an extremum in heave from what it is at the time of an extremum in pitch. It is shown in Appendix B that if the difference in horizontal ordinates of the midship's trace at maximum pitch and maximum heave are averaged with the corresponding differences at minimum pitch and minimum heave, the results give the phase displacement between pitch and heave.

Tables 1 through 7 and Figures 7 through 10 present the phase displacement results expressed in terms of the angle by which pitch leads heave.

For some test conditions the heaving and pitching motions were so small that the light traces appear to be only slightly perturbed from straight lines. The motions record from such a run is shown in Figure 11. Because the maxima and minima are so broad and ill-defined in such cases, the phase displacement may suffer a probable error as large as 10 to 15 percent. A more typical error would be about 5 percent.

DISCUSSION OF RESULTS

GENERAL FEATURES

With the exception of the tests performed with a tow weight consistent with a speed in still water corresponding to 10 knots for the full-scale ship, the agreement between the results obtained from the 5-ft and the 7.8-ft models was generally satisfactory.

With a tow weight for a still-water speed corresponding to 14 knots, the agreement in the speed reduction data was excellent for a wave steepness of 60, but there was a consistent tendency for the larger model to suffer a somewhat smaller speed reduction for a wave steepness of 40. For wave steepness ratios of both 60 and 40 the agreement between the two sets of results for heave, pitch, and phase displacement is quite good, since any of the deviations which occur could be accounted for in terms of errors in reading the photographic plates or the wave-height record. An interesting feature, however, is that whenever differences do occur in the motions results, the larger model usually exhibits the greater motion.

For the test results with a tow weight which would yield a still-water speed corresponding to 10 knots, the differences between the sets of data from the two models are quite striking. Only the differences which exist at wave lengths of one-half and three-fourths of the ship length could be explained in terms of data-reading errors. A more complete discussion of the poor agreement between the two sets of data follows.

POSSIBLE CAUSES FOR DISCREPANCIES

Reynolds Number

It is doubtful if the difference in Reynolds numbers between the two models at corresponding Froude numbers could account for the observed discrepancies. For the larger model, the Reynolds numbers relating to the conditions where difficulties were encountered are lower than the

Reynolds numbers associated with conditions which gave good results. For wave lengths of three-fourths ship length and above, the Reynolds numbers for the smaller model for the towing conditions in question are no smaller than the Reynolds numbers for other towing conditions where good agreement was achieved. Hence, the occurrence of any significant Reynolds number effects can be discounted.

Wave Reflection from Walls

Because the models are towed in a basin of finite width, the possibility exists that the wave train in the basin reflected from the model, or the waves generated by the motions of the model may propagate to the basin walls, be reflected there, and return to the center of the basin to influence the subsequent motion of the model. If, however, the model progresses with sufficient speed, it will have moved entirely out of the region of the reflections from the walls by the time they have propagated back to the center of the basin.

Assume that a wave whose length equals that of the incident wave is reflected from the model in a direction normal to the original direction of propagation. Require that the model travel at least its own length in the time necessary for the reflected wave to travel to the basin wall and back to the center of the basin. Then if W is the basin width and c is the wave celerity,

$$\frac{L}{v} \leqq \frac{W}{c/2}$$

Using the relation

$$c = \sqrt{g\lambda/2\pi}$$

then

$$v \geqq \frac{L}{2W}\sqrt{\frac{g\lambda}{2\pi}}$$

Denote the velocity for which the equality holds as v_{min} The waves

produced in consequence of the incident wave-induced motions of the model have the frequency of encounter and therefore (for towing in head seas) are of shorter wave length and propagate more slowly than the incident waves. The reflection of these disturbances from the basin walls thus imposes a less stringent restriction on the model velocity than the one given previously.

All the velocities observed for Model 3572-5a are greater than v_{min} for this model at all the wave lengths of concern. For Model 3572-8, v_{min} has the value

$$v_{min} = 0.522 \sqrt{\lambda}$$

where v_{min} is given in knots for λ in feet. Table 8 compares v_{min} with the average velocities observed for Model 3572-8 for the various test conditions at all five wave lengths used.

It can be seen from Table 8 that only for $v_s = 1.35$ (10 knots full scale) is v significantly smaller than v_{min}; this is true only for the three longer wave lengths. These conditions, however, are precisely the ones for which such poor agreement with the results for the small model were manifested. Yet at worst only the after third of the model would have been subjected to the first reflections from the walls, and it hardly seems reasonable to ascribe such pronounced differences in the behavior of the two models to what seems to be such a moderate influence. Thus, while wave reflections from the walls must bear some of the blame, a more profound cause for the observed discrepancies should be sought.

Towing System Dynamics

In Reference 1 the dynamics of the gravity dynamometer used for the present investigation were examined, and it was found that the towing system possessed one or two natural frequencies that were likely to coincide with a frequency of encounter a model might experience while being towed. To explore the possibility of such an occurrence in the test reported here, the results of Reference 1 were applied to the dynamometer in the several configurations of interest. Most of the preliminary tests

on Model 3572-5A were run with a silk towline installed, although this was replaced by a nylon towline before any of the runs for final data were recorded. The natural frequencies of the dynamometer while towing Model 3572-5A were calculated for both types of towline. Model 3572-8 was towed with a nylon line only, and so this case was the only one calculated. With two exceptions all dimensions and physical properties of the dynamometer components could be taken directly from Tables 1 and 2 of Reference 1. The length of the wire which joins the ends of the towline and to which the towing bracket is attached was 7.77 ft in place of the 6.80-ft wire installed at the time of the measurements of Reference 1. Also, because of a change in the wave absorber installation, the model could start its run closer to the wave absorber end of the basin during the tests reported here than was possible at the time of the investigation of Reference 1. As a consequence of these changes, the quantities denoted by δ_1, δ_2, and δ_o in Reference 1 should have their values changed to 0.1660, -0.0924, and 0.0609, respectively, and $\delta_{o\downarrow}$ should be changed to 0.0114 for Model 3572-5A and 0.0113 for Model 3572-8.

The natural frequencies of the dynamometer are a function of the instantaneous location of the model along the basin. For this reason the frequencies are calculated for both the minimum and maximum values of $(1/\rho_1 + 1/\rho_2)$ encountered during the recorded part of a run, where $(1/\rho_1 + 1/\rho_2)$ is a position parameter employed in Reference 1. In terms of an alternate position parameter, ρ, also defined in Reference 1, $(1/\rho_1 + 1/\rho_2)_{min}$ occurs at $\rho = (1 - \delta_1 + \delta_2)/2 = 0.3708$ and $(1/\rho_1+1/\rho_2)_{max}$ occurs at $\rho = 0.2100$, when the model has just completed its run through the test section of the basin.

Reference 1 gives the five natural frequencies of the towing system as the solution of a quintic equation. It also gives a very satisfactory approximation which yields the two highest natural frequencies as the solution of a quadratic and the three lowest frequencies as the solutions of a cubic. Table 9 lists the natural frequencies of the dynamometer in all the configurations mentioned, as calculated from the combination of cubic and quadratic equations. The two highest frequencies are functions of the tow weights used, and so results are quoted for the three different

tow weights employed with Model 3572-5A, and for the two different tow weights used with Model 3572-8. Half of the cases were recalculated from the quintic to test the worth of the approximate solution. In every case, the results were in agreement to three significant figures.

To perceive the applicability of the above calculations to the model experiments, the experiments will be examined for any unusual features, and these features will be classified according to the frequency of encounter, i.e., the forcing frequency.

Data for Model 3572-5A at a wave length of 1.5 ship length and V_s = 10 knots is missing. This is because, during the preliminary tests, the model exhibited an exaggerated oscillation in surge while being towed, actually changing its direction of motion at each cycle. The oscillations of the drive pulley were even more grossly amplified, thus making it quite impossible to measure an average speed of advance. By extrapolating the speed of advance at a wave length of 1.5 the model length from V_s = 18 and 14 knots to V_s = 10 knots, the speed of advance is estimated to be 0.93 V_s. This leads to a frequency of encounter ν_e = 1.05 cps. The calculated results for Model 3572-5A with silk towline give the lowest natural frequency in the range ν_n = 1.01 to ν_n = 1.02 cps. Thus the phenomenon described can be attributed to a resonance of the towing system. Unfortunately, the investigation reported here preceded the work of Reference 1, or it would have been realized that the later change to a nylon towline would have made it possible to accumulate data normally at the troublesome condition. The peculiarity just described was the only one observed with the smaller model.

Unusual features in the data from the larger model were observed, as mentioned before, for the three longer wave lengths with V_s corresponding to 10 knots. The frequencies of encounter encompassed by these conditions range from ν_e = 0.84 to ν_e = 1.06 cps. The location of the resonance within this range is not clear. The calculations for Model 3572-8 with nylon towline give the lowest natural frequency, ν_n = 0.81 cps. It is conceivable, though not in itself convincing, that the resonance occurs

at about 0.81 cps and extends its effects as far as 1.06 cps because of a large width of the resonant peak.

Another unusual effect which occurs with Model 3572-8 is not shown in the final recorded data, but affords a clear indication of the actual location of the resonance. It was noticed in the detailed motions data taken from the photographic plates that some of the pitch records showed sharp variations in the maximum or minimum pitch angles between adjacent cycles. To be certain that no variations due to reading errors could affect the conclusions, only those records were considered for which the maximum difference between consecutive extrema in pitch angles exceeded 15 min. The test conditions for which this maximum difference $\Delta\theta$ exceeded 15 min. included three conditions for which V_s corresponds to 14 knots as well as two conditions for which V_s equals 10 knots. The conditions are identified and the appropriate values of $\Delta\theta$ and $\Delta\theta/\theta$ are listed in Table 10. The values of $\Delta\theta/\theta$ averaged for the two tests (in one case, three tests) at each condition are plotted as a function of frequency of encounter in Figure 12. The curve in Figure 12 rises distinctly at the end of the plot where $\nu_e = 0.84$ cps.

This competes the list of unusual features observed with the two models. In every case the abnormality can be attributed to the proximity of a nuatural frequency of the dynamometer. There is no reason to doubt that a resonance with the dynamometer could cause discrepancies of the observed magnitude. Two details, however, require explanation. First, although every case of a frequency of encounter near the lowest natural frequency of the towing system led to some sort of difficulty, many of the test conditions were run near the next-to-lowest natural frequency of the dynamometer with no observable ill effects. Second, the resonant behavior of Model 3572-5A was so much more violent than the behavior of Model 3572-8 at its resonance.

Without solving the equations of motion of the dynamometer, it is possible to describe the separate modes of motion of the system by noting the dependence on the various inertial and elastic elements of the system

of the natural frequency corresponding to each mode of motion. For example, because the two highest natural frequencies depend on the tow weights and the properties of the tow pan wires, and to a slight extent on the moment of inertia of the drive pulley, the corresponding modes of motion involve a vibration of the tow weights on their supporting wires, accompanied by a slight oscillation of the drive pulley and no discernible motion of the rest of the system. Also, because the third or intermediate natural frequency is determined primarily by the properties of the towing bracket and the elasticity of the towline, the corresponding mode of motion is one in which the pulleys and model remain almost stationary while the towing bracket oscillates about its pivot in the model.

The modes of motion of the two lowest frequencies cannot be described as readily as the other three modes, but their general nature can be examined by varying the properties of each of the inertial and elastic elements in turn and by finding how the resulting natural frequencies change. For these calculations it is sufficient to use an approximation from Reference 1 which gives the two lowest natural frequencies as the solutions of a quadratic equation. For the next-to-lowest frequency the program of variation of the constants of the system reveals a strong dependence on the towline elasticity, a moderate dependence on the moments of inertia of the pulleys, a very slight dependence on the towing bracket properties, and almost no dependence on the mass of the model. This mode of motion may then be envisioned as an opposite (out-of-phase) oscillation of the pulleys that involves little motion of the towing bracket and almost no motion of the model. A resonance with this natural frequency then might give a speed deviation record with amplified oscillation, but should not affect average speed of advance or the motions records of the model.

The lowest natural frequency shows a strong dependence on the towline elasticity and the moments of inertia of both pulleys. The dependence on towing bracket properties is moderate; the dependence on the model mass varies from moderate to slight. To be more quantitative,a 20 percent decrease in the mass of the model produces a 2.1 percent increase in the lowest natural frequency for Model 3572-5A and a 0.6 percent increase in

this frequency for Model 3572-8. Thus the mode of motion corresponding to the lowest natural frequency is the only mode in which the model participates appreciably, and the degree of this participation is greater the smaller the mass of the model.

The motion of the system for its lowest natural frequency is the most complicated. In this mode the model surges, accompanied by a rotation of the towing bracket and rotation of the pulleys similar to that which is obtained in the next-to-lowest model of motion. However, because of the model motion, the deflection of the pulleys would be expected to be more extreme in the lowest mode than in the second mode, which would account for the increased dependence of the lowest natural frequency on the pulley properties. This would also lead to oscillations of the drive pulley which would have a more drastic effect on speed measurements in the lowest mode than in the second mode.

A final comment is that although the water level in the basin was maintained at the proper level for the tests discussed here, it was permitted to fall below the usual level during the measurements reported in Reference 1. The only effect would be in the adjustment of the towing bracket. If the water level is raised, the towing bracket arms must be spread and the overall height reduced. A 1-in. increase in the water level would thus cause an increase of about 15 percent in the Σ/α_2 is a quantity defined in Reference 1 which gives a significant measure of the towing bracket properties. If this change is incorporated into the calculations for the lowest natural frequencies, the result for Model 3572-5A with silk towline is now $\nu_n = 1.05$ cps and for Model 3572-8 with nylon towline $\nu_n = 83$ cps. These results compare favorably with the estimated locations of the resonances.

CONCLUDING REMARKS

Although the experimental investigation reported here of the effects

of scale on ship model motions in waves was of very modest scope, it served to demonstrate the importance of towing system dynamics in wave tests. Discrepancies in the data from the two models occurred if and only if the frequency of encounter of the model was near the lowest natural frequency of the gravity dynamometer neglecting reading errors. It was concluded that Reynolds number differences between the two models had no discernible effects. Any effect on the larger model caused by the reflections of waves from the wall was masked by the resonant effects and could not be evaluated separately. Thus, within the limited scope of the experiments, no scale effects were found which were attributable to the model itself.

The method of recording and reading motion data described in this report is not currently in use at TMB. The photographic method has since been replaced by electronic techniques where the signals are recorded on tape and/or chart paper. This latter method makes the task of data analysis less tedious.

APPENDIX A

MEASUREMENT OF HEAVE

Let the origin of time be chosen so that the heaving motion of the center of gravity of the model can be written as

$$z = a \sin \omega t$$

The pitching of the model can then be described by

$$\phi = \theta \sin (\omega t - \alpha)$$

If ℓ is the distance that the midship's light is elevated above the center of gravity, then the vertical motion of this light (measured from the mean center of gravity location) is

$$y = a \sin \omega t + \ell \cos \phi$$

If the heave measurement is to be obtained from the amplitude of the motion of the midship's light, then it is the extrema of the y curve which are of interest.

$$\frac{dy}{dt} = 0 = \omega a \cos \omega t - \ell \omega \theta \cos (\omega t - \alpha) \sin \phi$$

Since θ may be assumed to be small, let

$$\sin \phi \approx \theta \sin (\omega t - \alpha)$$

Hence

$$a \cos \omega t = \ell \theta^2 \sin (\omega t - \alpha) \cos (\omega t - \alpha)$$

Let $\omega t = \frac{\pi}{2} + \delta$ where δ is small. Then

$$\sin \omega t \approx 1$$

$$\cos \omega t \approx -\delta$$

$$\sin (\omega t-\alpha) \approx \cos \alpha + \delta \sin \alpha$$

$$\cos (\omega t-\alpha) \approx -\delta \cos \alpha + \sin \alpha$$

When substituted into Equation [1], the result is

$$\delta = -\frac{\ell\theta^2}{a} \sin \alpha \cos \alpha$$

Now let $\omega t = -\frac{\pi}{2}+\epsilon$ in Equation [1]. Then it is found that

$$\epsilon = \frac{\ell\theta^2}{a} \sin \alpha \cos \alpha$$

The quantity required is $y_{max}-y_{min}$ where

$$y_{max} = a \sin (\tfrac{\pi}{2}+\delta) + \ell \cos [\theta \sin (\tfrac{\pi}{2}+\delta-\alpha)]$$
$$y_{min} = a \sin (-\tfrac{\pi}{2}+\epsilon) + \ell \cos [\theta \sin (-\tfrac{\pi}{2}+\epsilon-\alpha)]$$

Since

$$\epsilon = -\delta$$

$$y_{max} - y_{min} = 2a \sin (\tfrac{\pi}{2}+\delta)$$

$$+ 2\ell \sin [\theta \sin (\tfrac{\pi}{2}+\delta) \cos \alpha] \sin [\theta \cos (\tfrac{\pi}{2}+\delta) \sin \alpha]$$

and within second-order terms, this gives

$$y_{max} - y_{min} = 2a$$

APPENDIX B

MEASUREMENT OF PHASE DISPLACEMENT

Let x be a horizontal ordinate (increasing in the direction of tow) and let the subscripts p refer to pitch, h to heave, r to real value (i.e., referring to values taken from the trace made by the midship's light.) Bow up pitch angles are positive. Then the horizontal ordinate of the center of gravity at maximum pitch is

$$x_{rp} = x_{ap} + \ell \sin \phi_p \qquad [2]$$

At minimum pitch it is

$$x_{rp}' = x_{ap}' + \ell \sin \phi_p' \qquad [3]$$

At maximum heave

$$x_{rh} = x_{ah} + \ell \sin \phi_h \qquad [4]$$

and at minimum heave

$$x_{rh}' = x_{ah}' + \ell \sin \phi_h' \qquad [5]$$

Then if the phase displacement between pitch and heave is expressed by

$$\alpha = 2\pi \left[\frac{(x_{rh}-x_{rp}) + (x_{rh}'-x_{rp}')}{2\lambda} \right]$$

it follows from Equations [2] through [5] that if $\phi_h = -\phi_h'$ and $\phi_p = -\phi_p'$, then

$$\alpha = \frac{\pi}{\lambda}[(x_{ah}-x_{ap}) + (x_{ah}'-x_{ap}')]$$

If, however, there exists a nonzero average pitching angle of amount ϵ, then

$$\phi_p = -\phi_p' + 2\epsilon$$

When no trim exists,

$$\phi_h = \phi_p \cos \alpha \text{ and } \phi_h' = \phi_p' \cos \alpha$$

but the angle ϵ

$$\phi_h = \epsilon + (\phi_p - \epsilon) \cos \alpha$$

$$\phi_h' = \epsilon + (\phi_p' - \epsilon) \cos \alpha$$

$$= \epsilon - (\phi_p - \epsilon) \cos \alpha$$

Hence

$$\sin \phi_h + \sin \phi_h' = 2 \sin \epsilon \cos [(\phi_p - \epsilon) \cos \alpha]$$

$$\approx 2\epsilon$$

for small pitching angles. Also,

$$\sin \phi_p + \sin \phi_p' \approx 2\epsilon$$

Thus, even when a nonzero average pitching angle exists,

$$\alpha = \frac{\pi}{\lambda} [(x_{ah} - x_{ap}) + (x_{ah}' - x_{ap}')]$$

REFERENCES

1. Reiss, H. R., "The Dynamics of a Gravity Towing System," David Taylor Model Basin Report 1040 (Jul 1957).

2. Campbell, W. S., "An Electronic Wave-Height Measuring Apparatus," David Taylor Model Basin Report 859 (Oct 1953).

3. Baier, L. A., "The 1939 Report of the American Towing Tank Conference," Transactions of The Society of Naval Architects and Marine Engineers, Vol 47 (1939).

4. Landweber, L., "Tests of a Model in Restricted Channels," Experimental Model Basin Report 460 (May 1939).

5. Reiss, H. R., "A Procedure to Impart Specified Dynamical Properties to Ship Models," David Taylor Model Basin Report 986 (Mar 1956).

6. Thews, J. G. and Landweber, L., "Resistance Tests in the U. S. Eighty-Foot Model Basin," Unpublished.

Figure 1 - 5-Foot SAN FRANCISCO Model

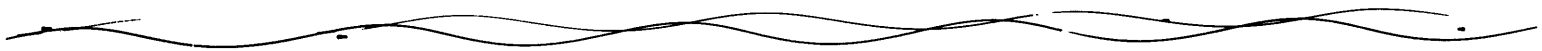

Figure 2 - Sample Motions Record for Model 3572-8 in Waves of $\lambda/L = 1.25$ and $\lambda/H = 60$ for a Thrust Corresponding to 14-knot Still-Water Speed

Figure 3 - Sample Motions Record for Model 3572-8 in Waves of $\lambda/H = 60$ for a Thrust Corresponding to 10-knot Still-Water Speed

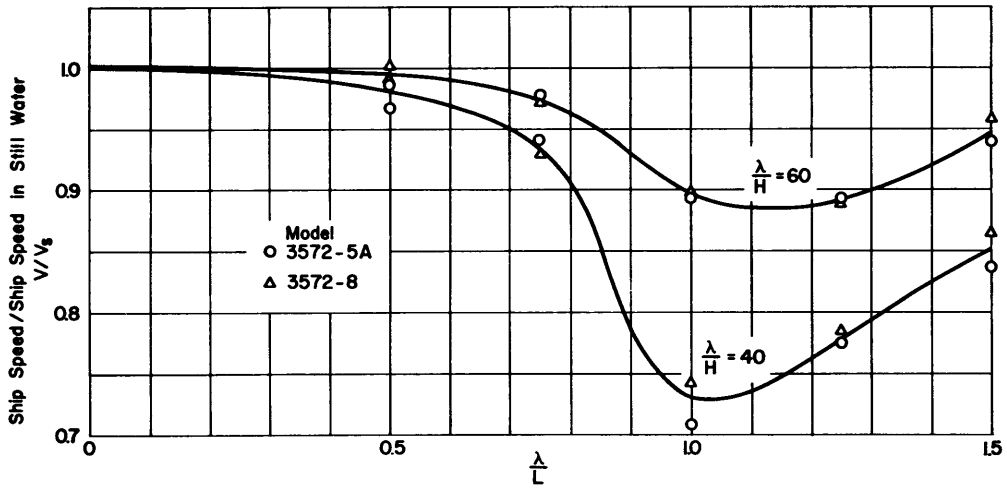

Figure 4 - Speed Reduction in Waves for Thrust Corresponding to 14-knot Still-Water Speed

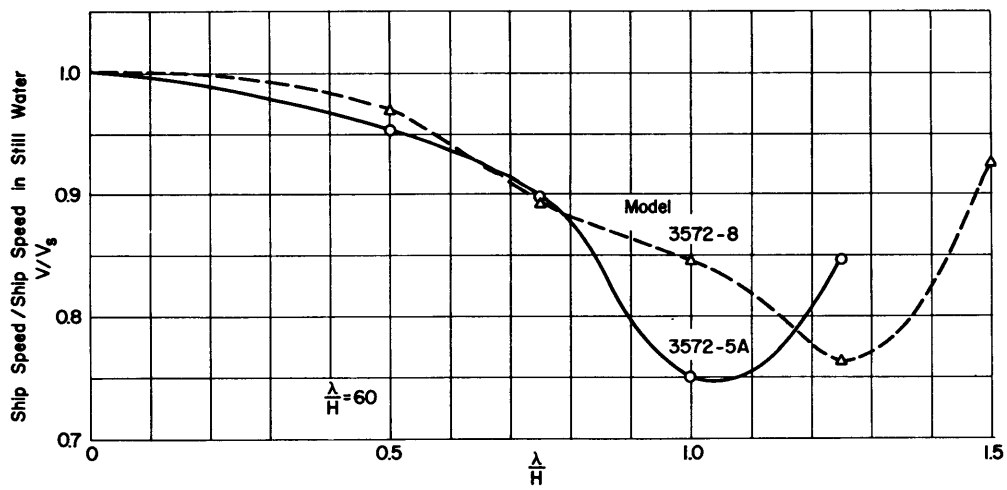

Figure 5 - Speed Reduction in Waves for Thrust Corresponding to 10-knot Still-Water Speed

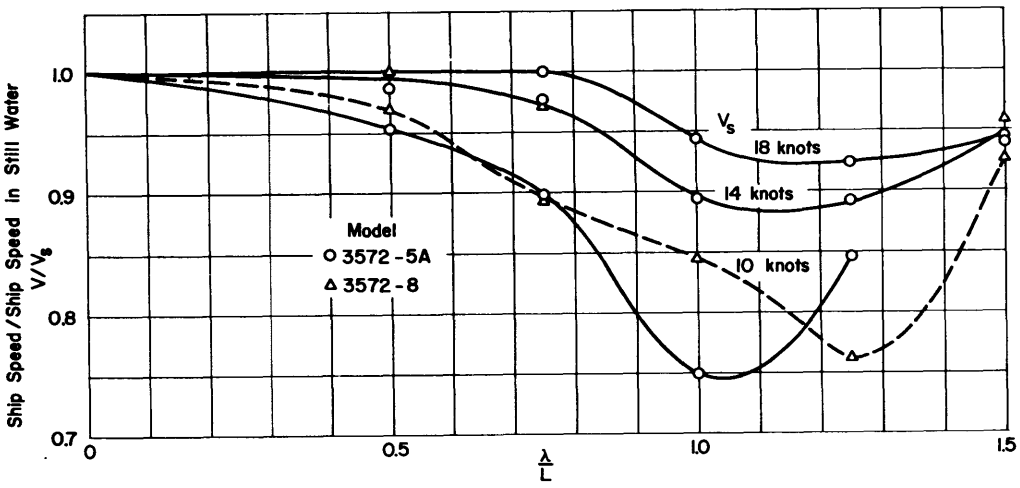

Figure 6 - Speed Reduction in Waves for $\lambda/H = 60$

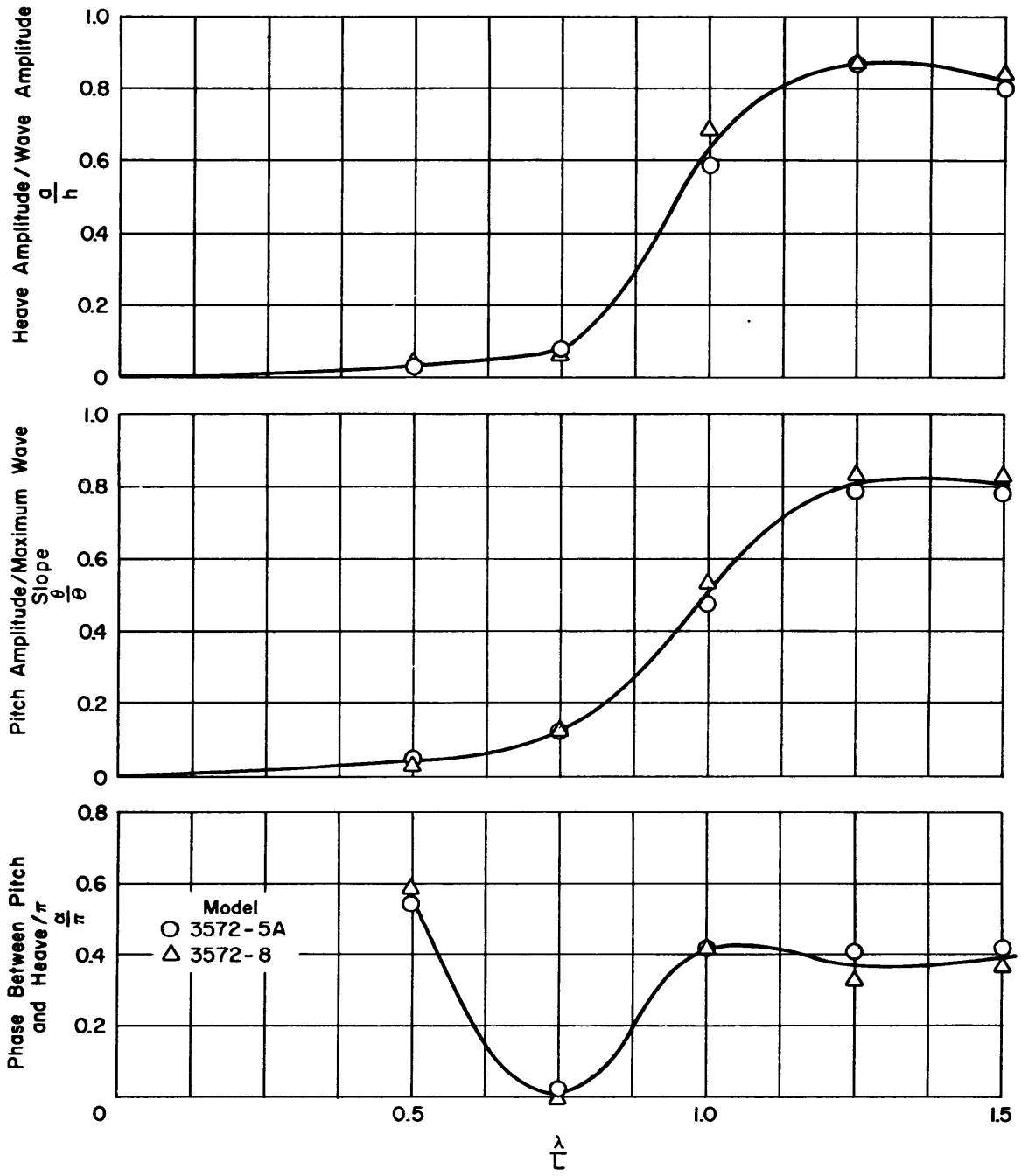

Figure 7 - Ship Motions in Waves of $\lambda/H = 60$ for a Thrust Corresponding to 14-knot Still-Water Speed

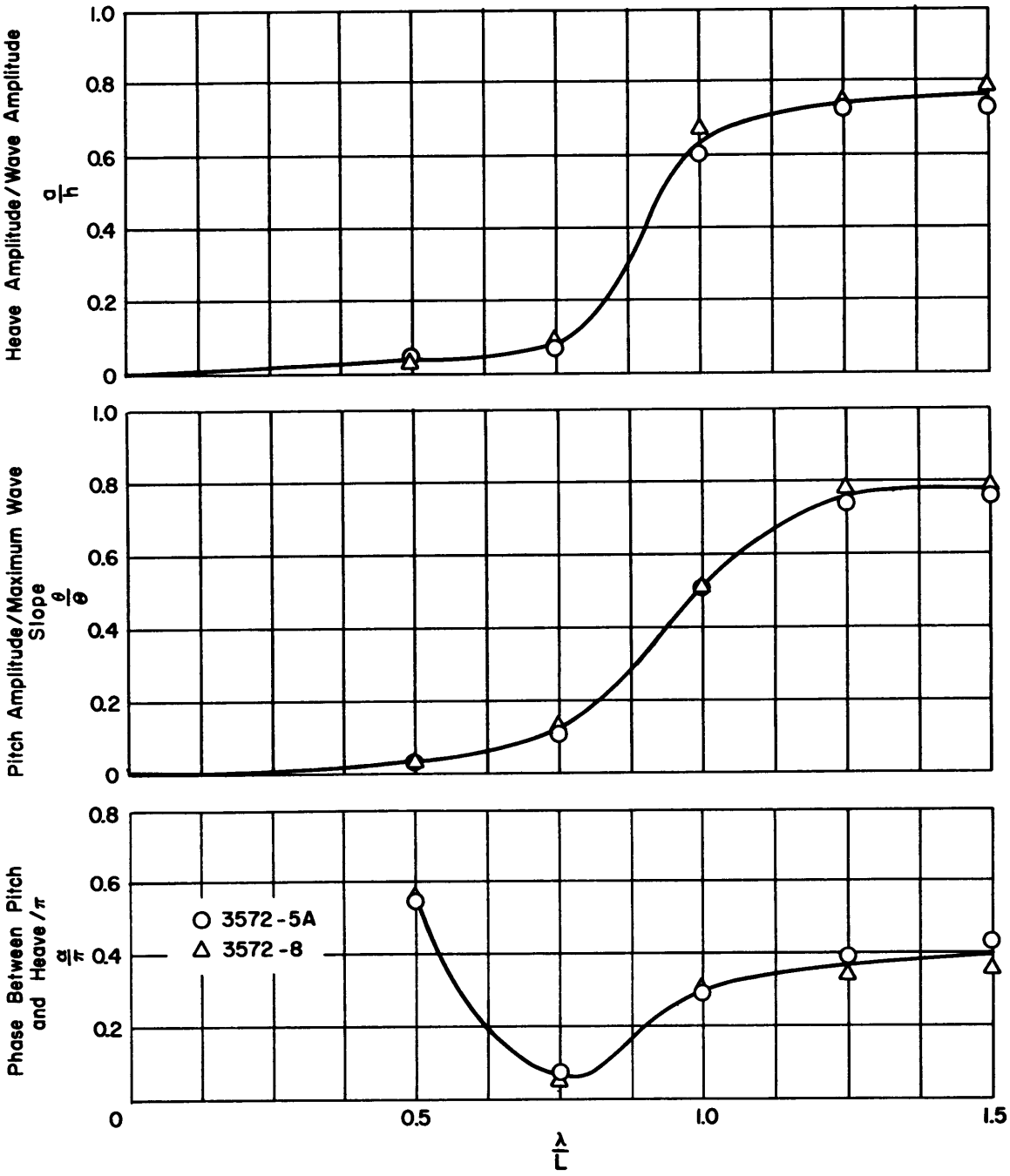

Figure 8 - Ship Motions in Waves of $\lambda/H = 40$ for a Thrust Corresponding to 14-knot Still-Water Speed

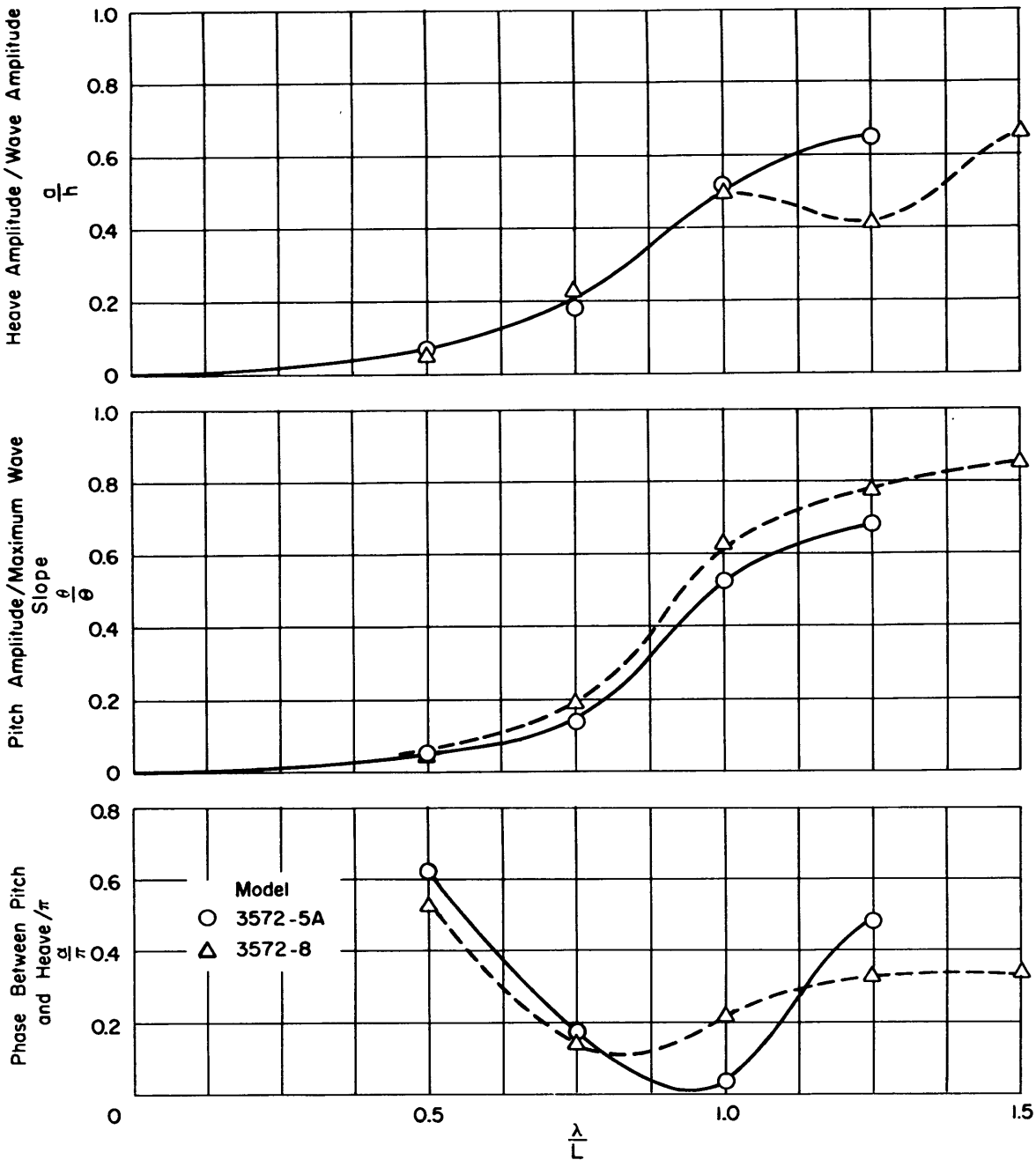

Figure 9 - Ship Motions in Waves of $\lambda/H = 60$ for a Thrust Corresponding to 10-knot Still-Water Speed

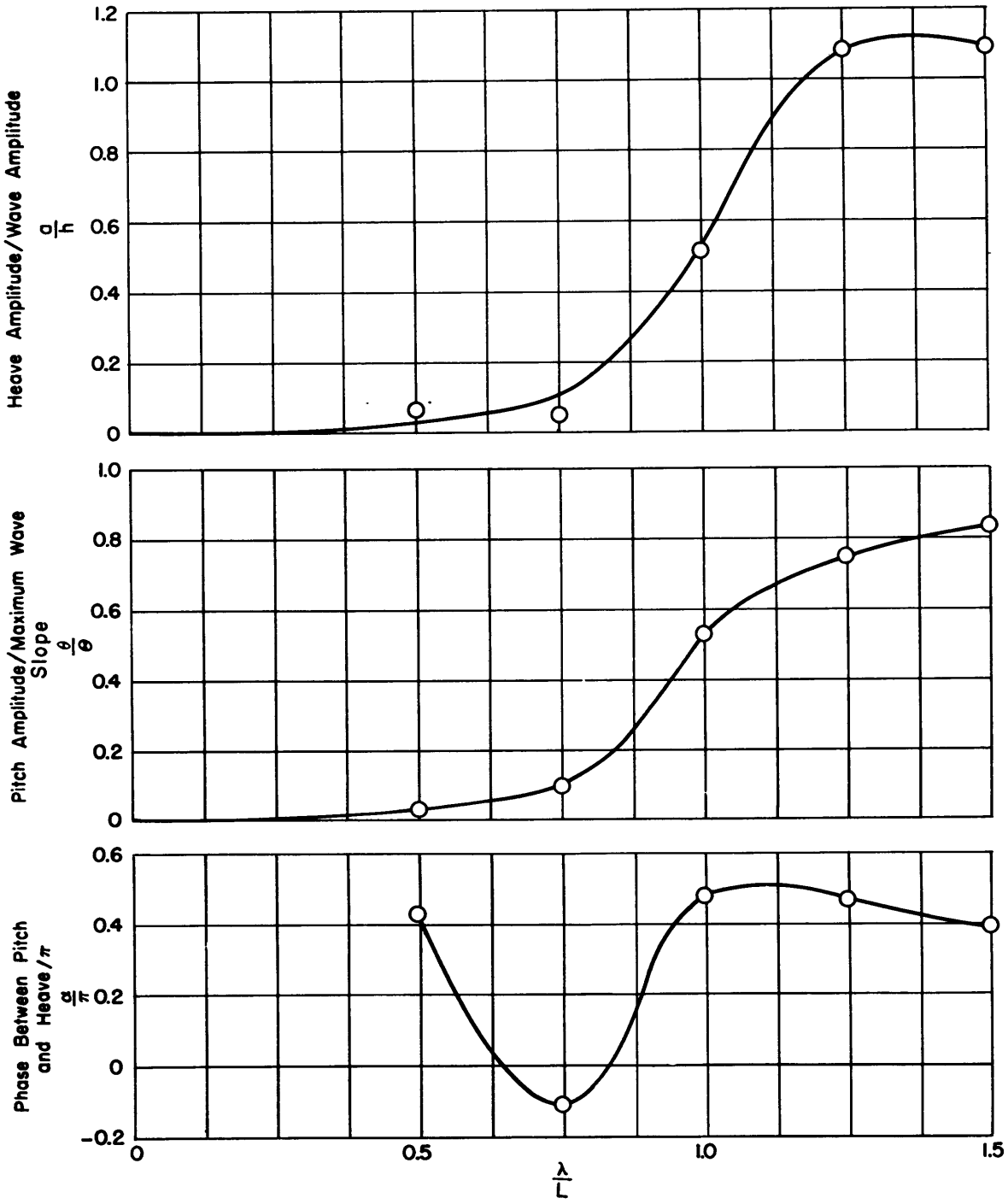

Figure 10 - Ship Motions in Waves of $\lambda/H = 60$ for a Thrust Corresponding to 18-knot Still-Water Speed

Figure 11 - Example of Small Amplitude Motions Record. Model 3572-8 in Waves of $\lambda/L = 0.5$ and $\lambda/H = 60$ for a Thrust Corresponding to 10-knot Still-Water Speed

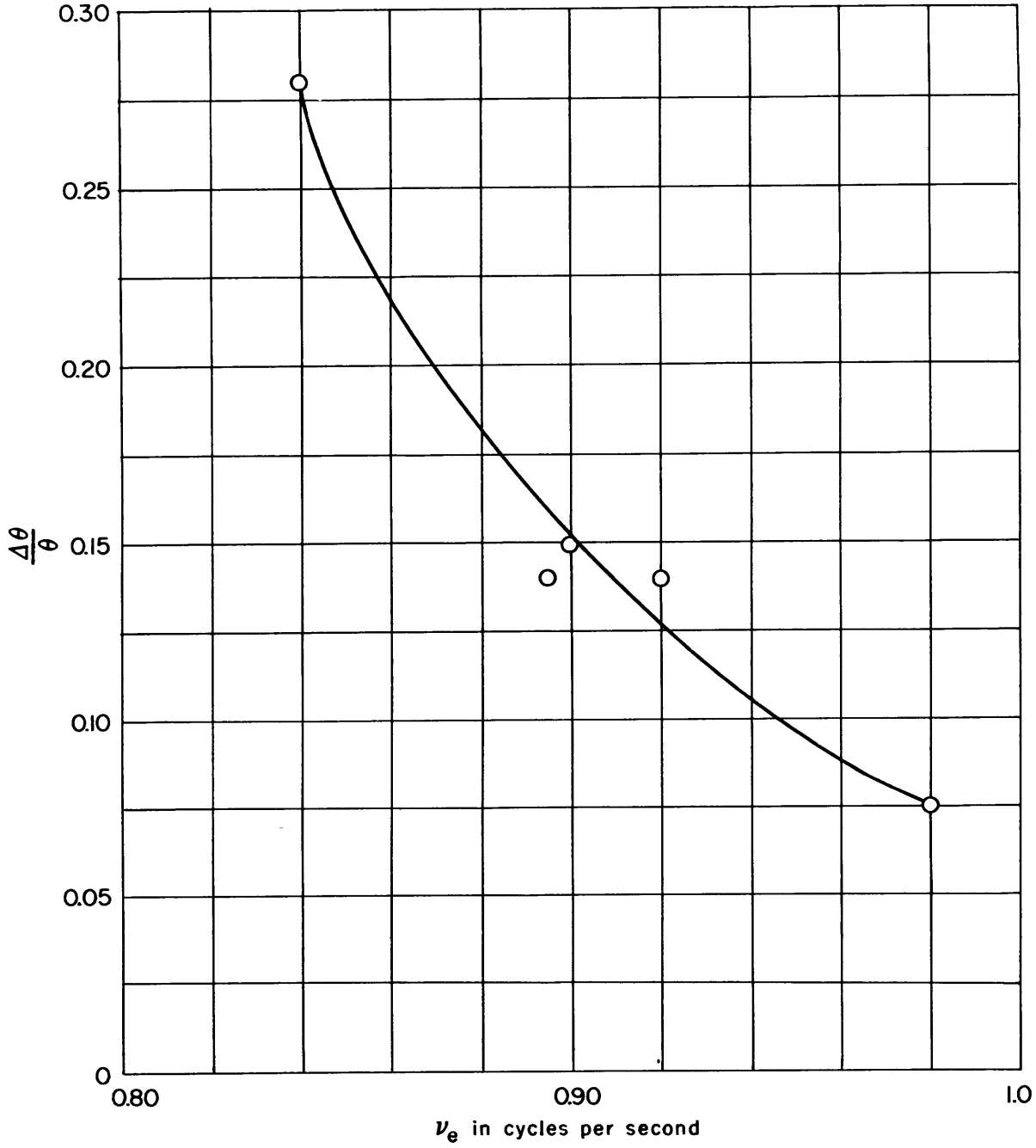

Figure 12 - Fluctuations in Pitch Angle, Model 3572-8

TABLE 1

Data for Model 3572-5A, V_s = 14 Knots, $\frac{\lambda}{H} = 60$

$\frac{\lambda}{L}$	H in.	v knots	ν_e cyc/sec	a in.	$\frac{a}{h}$	θ min	$\frac{\theta}{\Theta}$	$\frac{\alpha}{\pi}$
1.5	1.53	1.42	1.15	0.6033	0.789	140.4	0.765	0.408
	1.46	1.42	1.15	0.5970	0.818	140.1	0.800	0.417
1.25	1.21	1.35	1.27	0.5292	0.875	137.8	0.791	0.435
	1.23	1.34	1.27	0.5346	0.869	138.9	0.784	0.376
1.0	1.06	1.34	1.46	0.3125	0.590	91.0	0.477	0.428
	1.03	1.36	1.47	0.3079	0.598	88.2	0.476	0.429
0.75	0.72	1.48	1.83	0.0250	0.0694	20.8	0.120	-0.005
	0.74	1.47	1.83	0.0272	0.0735	21.3	0.120	0.041
0.5	0.51	1.49	2.44	0.0110	0.0432	7.6	0.041	0.514
	0.47	1.49	2.44	0.0105	0.0447	7.3	0.043	0.571

TABLE 2

Data for Model 3572-5A, V_s = 14 Knots, $\frac{\lambda}{H} = 40$

$\frac{\lambda}{L}$	H in.	v knots	ν_e cyc/sec	a in.	$\frac{a}{h}$	θ min	$\frac{\theta}{\Theta}$	$\frac{\alpha}{\pi}$
1.5	2.29	1.25	1.11	0.8546	0.746	206.4	0.751	0.424
	2.24	1.20	1.10	0.8144	0.727	208.9	0.777	0.436
1.25	1.91	1.18	1.22	0.7034	0.737	202.6	0.737	0.409
	1.88	1.16	1.22	0.6885	0.732	201.2	0.743	0.368
1.0	1.50	1.07	1.37	0.4413	0.588	133.3	0.494	0.270
	1.42	1.07	1.37	0.4443	0.626	135.9	0.532	0.301
0.75	1.14	1.42	1.81	0.0397	0.0696	30.9	0.113	0.062
	1.12	1.42	1.81	0.0381	0.0680	27.1	0.101	0.088
0.5	0.76	1.46	2.42	0.0185	0.0487	10.2	0.037	0.532
	0.73	1.46	2.42	0.0169	0.0463	9.2	0.035	0.557

TABLE 3

Data for Model 3572-5A, V_s = 10 Knots, $\frac{\lambda}{H} = 60$

$\frac{\lambda}{L}$	H in.	v knots	ν_e cyc/sec	a in.	$\frac{a}{h}$	θ min	$\frac{\theta}{\Theta}$	$\frac{\alpha}{\pi}$
1.25	1.26	0.92	1.16	0.4177	0.663	124.7	0.687	0.479
	1.26	0.91	1.15	0.4062	0.646	122.6	0.675	0.484
1.0	1.00	0.81	1.29	0.2583	0.517	94.0	0.522	0.014
	0.98	0.81	1.29	0.2550	0.520	93.8	0.532	0.050
0.75	0.77	0.97	1.60	0.0739	0.192	27.0	0.146	0.163
	0.79	0.97	1.60	0.0686	0.174	25.5	0.134	0.179
0.5	0.50	1.03	2.13	0.0205	0.0820	11.1	0.0614	0.612
	0.49	1.03	2.13	0.0159	0.0649	10.1	0.0572	0.633

TABLE 4

Data for Model 3572-5A, V_s = 18 Knots, $\frac{\lambda}{H} = 60$

$\frac{\lambda}{L}$	H in.	v knots	ν_e cyc/sec	a in.	$\frac{a}{h}$	θ min	$\frac{\theta}{\Theta}$	$\frac{\alpha}{\pi}$
1.5	1.46	1.82	1.24	0.8283	1.136	150.8	0.861	0.386
	1.54	1.82	1.24	0.8047	1.045	150.8	0.816	0.399
1.25	1.28	1.79	1.39	0.7071	1.105	138.3	0.750	0.467
	1.26	1.78	1.39	0.6781	1.076	135.7	0.748	0.469
1.0	1.04	1.82	1.63	0.2816	0.542	102.6	0.548	0.495
	1.08	1.82	1.63	0.2676	0.496	100.1	0.515	0.467
0.75	0.77	1.93	2.04	0.0177	0.0461	17.7	0.0958	−0.120
	0.73	1.93	2.04	0.0220	0.0603	18.1	0.103	−0.105
0.5	0.48	1.93	2.73	0.0153	0.0638	4.0	0.023	0.446
	0.48	1.93	2.73	0.0151	0.0629	4.4	0.026	0.412

TABLE 5

Data for Model 3572-8, V_s = 14 Knots, $\frac{\lambda}{H} = 60$

$\frac{\lambda}{L}$	H in.	v knots	ν_e cyc/sec	a in.	$\frac{a}{h}$	θ min	$\frac{\theta}{\Theta}$	$\frac{\alpha}{\pi}$
1.5	2.30	1.87	0.93	0.9777	0.850	149.7	0.846	0.363
	2.40	1.80	0.92	0.9867	0.823	149.2	0.808	0.360
	2.33	1.77	0.91	0.9934	0.853	147.1	0.821	0.371
1.25	1.96	1.72	1.02	0.8514	0.869	152.3	0.842	0.315
	1.98	1.64	1.01	0.8730	0.882	149.9	0.820	0.331
1.0	1.59	1.70	1.18	0.5475	0.689	96.6	0.527	0.403
	1.59	1.69	1.18	0.5458	0.687	97.7	0.533	0.410
0.75	1.11	1.84	1.47	0.0418	0.0753	22.0	0.129	0.023
	1.17	1.83	1.46	0.0390	0.0667	21.4	0.119	−0.060
0.5	0.75	1.89	1.96	0.0232	0.0619	6.8	0.039	0.614
	0.75	1.89	1.96	0.0212	0.0565	5.7	0.033	0.562

TABLE 6

Data for Model 3572-8, V_s = 14 Knots, $\frac{\lambda}{H} = 40$

$\frac{\lambda}{L}$	H in.	v knots	ν_e cyc/sec	a in.	$\frac{a}{h}$	θ min	$\frac{\theta}{\Theta}$	$\frac{\alpha}{\pi}$
1.5	3.51	1.65	0.90	1.392	0.793	214.9	0.796	0.343
	3.55	1.62	0.89	1.396	0.786	215.0	0.787	0.367
1.25	2.99	1.47	0.98	1.105	0.739	212.8	0.771	0.337
	2.93	1.49	0.98	1.099	0.750	214.1	0.792	0.347
1.0	2.36	1.40	1.11	0.7912	0.671	139.9	0.514	0.307
	2.35	1.40	1.11	0.7999	0.681	141.9	0.523	0.303
0.75	1.76	1.76	1.44	0.0736	0.0836	36.5	0.135	0.026
	1.75	1.75	1.44	0.0720	0.0823	37.3	0.139	0.090
0.5	1.15	1.87	1.96	0.0186	0.0323	8.2	0.031	0.508
	1.13	1.87	1.96	0.0214	0.0379	10.4	0.040	0.619

TABLE 7

Data for Model 3572-8, V_s = 10 Knots, $\frac{\lambda}{H} = 60$

$\frac{\lambda}{L}$	H in.	v knots	ν_e cyc/sec	a in.	$\frac{a}{h}$	θ min	$\frac{\theta}{\Theta}$	$\frac{\alpha}{\pi}$
1.5	2.35	1.25	0.84	0.7818	0.665	154.5	0.855	0.342
	2.36	1.25	0.84	0.7846	0.665	155.8	0.858	0.324
1.25	2.00	1.03	0.90	0.4272	0.427	145.4	0.788	0.314
	2.01	1.03	0.90	0.4111	0.409	141.0	0.760	0.330
1.0	1.58	1.14	1.06	0.3879	0.491	115.6	0.634	0.206
	1.59	1.14	1.06	0.3954	0.497	114.5	0.624	0.232
0.75	1.12	1.22	1.29	0.1197	0.214	30.5	0.177	0.131
	1.11	1.19	1.28	0.1302	0.235	34.7	0.203	0.145
0.5	0.83	1.31	1.71	0.0227	0.0547	9.6	0.050	0.485
	0.74	1.31	1.71	0.0196	0.0530	9.0	0.053	0.581

TABLE 8

V_{min} for Model 3572-8

		V_s = 14 Knots $\frac{\lambda}{H} = 60$	V_s = 14 Knots $\frac{\lambda}{H} = 40$	V_s = 10 Knots $\frac{\lambda}{H} = 60$
$\frac{\lambda}{L}$	v_{min} knots	v knots	v knots	v knots
1.5	1.79	1.81	1.64	1.25
1.25	1.63	1.68	1.48	1.03
1.0	1.46	1.70	1.40	1.14
0.75	1.26	1.84	1.76	1.21
0.5	1.03	1.89	1.87	1.31

TABLE 9

Natural Frequencies of Dynamometer

	3572-5A, Nylon Line		3572-5A, Silk Line		3572-8, Nylon Line	
	$\rho = 0.3708$ ν_n cyc/sec	$\rho = 0.2100$ ν_n cyc/sec	$\rho = 0.3708$ ν_n cyc/sec	$\rho = 0.2100$ ν_n cyc/sec	$\rho = 0.3708$ ν_n cyc/sec	$\rho = 0.2100$ ν_n cyc/sec
	0.876	0.879	1.01	1.02	0.809	0.813
	1.39	1.42	1.78	1.82	1.39	1.42
	5.74	5.85	6.38	6.55	5.15	5.25
V_s = 10 knots	12.3	10.9	12.3	10.9	11.6	10.2
	16.8	22.3	16.8	22.3	18.0	23.9
V_s = 14 knots	11.8	10.5	11.8	10.5	10.7	9.58
	17.3	23.0	17.3	23.0	20.7	27.5
V_s = 18 knots	11.3	9.90	11.3	9.90	–	–
	18.8	25.0	18.8	25.0	–	–

TABLE 10

Maximum Fluctuation in Pitch Angle between Consecutive Cycles, Model 3572-8

	Test Conditions				
ν_e cyc/sec	V_s knots	$\frac{\lambda}{H}$	$\frac{\lambda}{L}$	$\Delta\theta$ min	$\frac{\Delta\theta}{\theta}$
0.84	10	60	1.5	44	0.28
0.895	14	40	1.5	31	0.14
0.90	10	60	1.25	22	0.15
0.92	14	60	1.5	21	0.14
0.98	14	40	1.25	16	0.075

INITIAL DISTRIBUTION

Copies

6 CHBUSHIPS
- 3 Tech Info (Code 335)
- 1 Tech Asst to Chief (Code 106)
- 1 Lab Mgt (Code 320)
- 1 Appl Sci (Code 342)

4 CHBUWEPS
- 2 Mine & Explosives (RUME)
- 2 Aero & Hydro Sec (RAAD-3)

1 CHONR, Fluid Dyn (Code 438)

1 CDR, NORVA, UERD (Code 280)

2 CDR, USNOL
- 1 Dr. Albert May

1 DIR, USNRL

2 DIR, NASA

3 DIR, Langley Res Ctr
- 1 Dr. C. Kaplan
- 1 Mr. F.L. Thompson

2 CDR, USNOTS, Underwater Ord Div, Pasadena

2 CDR, USNOTS, China Lake
- 1 Dr. E.O. Cooper

1 DIR, Natl BuStand
Attn: Dr. G.H. Keulegan

1 DIR, Defense Res & Eng

1 DIR, Oak Ridge Natl Lab, Oak Ridge

1 DIR, US Waterways Exp Sta

2 NNS & DD Co
- 1 Asst Naval Architect
- 1 DIR, Hydraulic Lab

2 DIR, Appl Phys Lab, Johns Hopkins Univ, Silver Spring, Md.

1 DIR, Daniel Guggenheim Aero Lab, CIT, Pasadena

1 DIR, Fluid Mech Lab, Columbia Univ

1 DIR, Fluid Mech Lab, Univ of California, Berkeley

4 DIR, Davidson Lab, SIT
- 1 Mr. Peters
- 1 Mr. E.V. Lewis

1 DIR, Dept of Civil & Sanitary Engin, Hydro Lab, MIT, Cambridge

1 DIR, Exptl Nav Tank, Univ of Michigan

1 DIR, Inst for Fluid Dyn & Appl Math, Univ of Maryland

1 DIR, Inst of Aero Sciences, New York

1 DIR, Fluid Mech Lab, Dept of Engin Mech, New York University

1 DIR, ORL, Penn State Univ

1 Admin, Webb Inst of Nav Arch

2 DIR, Iowa Inst of Hydraulic Res, State Univ of Iowa
- 1 Dr. L. Landweber

Copies

1 DIR, St. Anthony Falls Hydraulic Lab, Univ of Minnesota

1 Head, Dept of NAME, MIT

1 Hydro Lab, Attn: Exec Comm, CIT

10 CDR, ASTIA
Attn: TIPDR

2 The Martin Co, Baltimore
Attn: Engineering Library

1 Prof. M.A. Abkowitz, Dept of NAME, MIT

1 Convair Div of Genl Dyn Corp, San Diego
Attn: Mr. F.L. Thornbaugh, Sr Des Eng

1 Dr. H.W.E. Lerbs, Dir, Hamburg Model Basin

1 Prof. Dr.–Ing. G. Weinblum, Direktor Institut für Schiffbau der Universitat Hamburg, Germany

1 DIR, Nederlandsh Scheepsbouwkundig Proefstation, Haagsteeg 2, Wageningen

1 Prof. J.K. Lunde, Dir, Skipsmodelltanken, Trondheim

1 DIR, Res, British Shipbldg Res Assoc, London

1 Dr. F.H. Todd, Dir, Hydro Lab, Natl Phys Lab, Feltham, Middlesex, England

1 Dr. J. Okabe, Res Inst for Appl Mech, Kyushu Univ, Hakozaki-Machi, Fukuoka-shi, Japan

1 Supt, Admiralty Res Lab, Teddington, Middlesex, England

1 RADM M. Brard, Directeur, Bassin d'Essais des Carenes, Paris

1 Dr. L. Malavard, Office Natl d'Etudes et de Recherches Aeronautiques, Paris, France

1 Gen. Ing. U. Pugliese, Presidente, Istituto Nazionale per Studi ed Esperienze di Architettura Navale, Rome

1 Sr. M. Acevedo y Campoamor, Dir, Canal de Esperiencias Hidrodinamicas, El Pardo (Madrid)

1 Dr. J. Dieudonne, Directeur General, Institut de Recherches de la Construction Navale, Paris

1 Dir, Statens Skeppsprovningsanstalt, Goteborg

1 Chief Supt, Naval Res Estab, Halifax, Nova Scotia

8 ALUSNA, London

David Taylor Model Basin. Report 1039.
THE EFFECTS OF SCALE AND TOWING SYSTEM ON WAVE TESTS OF SMALL SHIP MODELS, by Howard R. Reiss. May 1961. v, 41p. illus., photos., graphs, refs. UNCLASSIFIED

To investigate experimentally the effect of scale on the motions of ship models in waves, two different scale models of the motor ship SAN FRANCISCO were tested. Although within the limits of the investigation there were no differences in the behavior of the models that could be ascribed to the effect of scale, several very noticeable effects were found that resulted from the dynamics of the towing system employed.

1. Ship models--Seaworthiness --Scale effects
2. Ship models--Motion-- Testing equipment
3. Ship models--Model TMB 3572-5A
4. Ship models--Model TMB 3572-8
5. SAN FRANCISCO (German Cargo ship)

I. Reiss, Howard R.

David Taylor Model Basin. Report 1039.
THE EFFECTS OF SCALE AND TOWING SYSTEM ON WAVE TESTS OF SMALL SHIP MODELS, by Howard R. Reiss. May 1961. v, 41p. illus., photos., graphs, refs. UNCLASSIFIED

To investigate experimentally the effect of scale on the motions of ship models in waves, two different scale models of the motor ship SAN FRANCISCO were tested. Although within the limits of the investigation there were no differences in the behavior of the models that could be ascribed to the effect of scale, several very noticeable effects were found that resulted from the dynamics of the towing system employed.

1. Ship models--Seaworthiness --Scale effects
2. Ship models--Motion-- Testing equipment
3. Ship models--Model TMB 3572-5A
4. Ship models--Model TMB 3572-8
5. SAN FRANCISCO (German Cargo ship)

I. Reiss, Howard R.

David Taylor Model Basin. Report 1039.
THE EFFECTS OF SCALE AND TOWING SYSTEM ON WAVE TESTS OF SMALL SHIP MODELS, by Howard R. Reiss. May 1961. v, 41p. illus., photos., graphs, refs. UNCLASSIFIED

To investigate experimentally the effect of scale on the motions of ship models in waves, two different scale models of the motor ship SAN FRANCISCO were tested. Although within the limits of the investigation there were no differences in the behavior of the models that could be ascribed to the effect of scale, several very noticeable effects were found that resulted from the dynamics of the towing system employed.

1. Ship models--Seaworthiness --Scale effects
2. Ship models--Motion-- Testing equipment
3. Ship models--Model TMB 3572-5A
4. Ship models--Model TMB 3572-8
5. SAN FRANCISCO (German Cargo ship)

I. Reiss, Howard R.

David Taylor Model Basin. Report 1039.
THE EFFECTS OF SCALE AND TOWING SYSTEM ON WAVE TESTS OF SMALL SHIP MODELS, by Howard R. Reiss. May 1961. v, 41p. illus., photos., graphs, refs. UNCLASSIFIED

To investigate experimentally the effect of scale on the motions of ship models in waves, two different scale models of the motor ship SAN FRANCISCO were tested. Although within the limits of the investigation there were no differences in the behavior of the models that could be ascribed to the effect of scale, several very noticeable effects were found that resulted from the dynamics of the towing system employed.

1. Ship models--Seaworthiness --Scale effects
2. Ship models--Motion-- Testing equipment
3. Ship models--Model TMB 3572-5A
4. Ship models--Model TMB 3572-8
5. SAN FRANCISCO (German Cargo ship)

I. Reiss, Howard R.

David Taylor Model Basin. Report 1039.
THE EFFECTS OF SCALE AND TOWING SYSTEM ON WAVE TESTS OF SMALL SHIP MODELS, by Howard R. Reiss. May 1961. v, 41p. illus., photos., graphs, refs. UNCLASSIFIED

To investigate experimentally the effect of scale on the motions of ship models in waves, two different scale models of the motor ship SAN FRANCISCO were tested. Although within the limits of the investigation there were no differences in the behavior of the models that could be ascribed to the effect of scale, several very noticeable effects were found that resulted from the dynamics of the towing system employed.

1. Ship models--Seaworthiness --Scale effects
2. Ship models--Motion-- Testing equipment
3. Ship models--Model TMB 3572-5A
4. Ship models--Model TMB 3572-8
5. SAN FRANCISCO (German Cargo ship)
I. Reiss, Howard R.

David Taylor Model Basin. Report 1039.
THE EFFECTS OF SCALE AND TOWING SYSTEM ON WAVE TESTS OF SMALL SHIP MODELS, by Howard R. Reiss. May 1961. v, 41p. illus., photos., graphs, refs. UNCLASSIFIED

To investigate experimentally the effect of scale on the motions of ship models in waves, two different scale models of the motor ship SAN FRANCISCO were tested. Although within the limits of the investigation there were no differences in the behavior of the models that could be ascribed to the effect of scale, several very noticeable effects were found that resulted from the dynamics of the towing system employed.

1. Ship models--Seaworthiness --Scale effects
2. Ship models--Motion-- Testing equipment
3. Ship models--Model TMB 3572-5A
4. Ship models--Model TMB 3572-8
5. SAN FRANCISCO (German Cargo ship)
I. Reiss, Howard R.

David Taylor Model Basin. Report 1039.
THE EFFECTS OF SCALE AND TOWING SYSTEM ON WAVE TESTS OF SMALL SHIP MODELS, by Howard R. Reiss. May 1961. v, 41p. illus., photos., graphs, refs. UNCLASSIFIED

To investigate experimentally the effect of scale on the motions of ship models in waves, two different scale models of the motor ship SAN FRANCISCO were tested. Although within the limits of the investigation there were no differences in the behavior of the models that could be ascribed to the effect of scale, several very noticeable effects were found that resulted from the dynamics of the towing system employed.

1. Ship models--Seaworthiness --Scale effects
2. Ship models--Motion-- Testing equipment
3. Ship models--Model TMB 3572-5A
4. Ship models--Model TMB 3572-8
5. SAN FRANCISCO (German Cargo ship)
I. Reiss, Howard R.

David Taylor Model Basin. Report 1039.
THE EFFECTS OF SCALE AND TOWING SYSTEM ON WAVE TESTS OF SMALL SHIP MODELS, by Howard R. Reiss. May 1961. v, 41p. illus., photos., graphs, refs. UNCLASSIFIED

To investigate experimentally the effect of scale on the motions of ship models in waves, two different scale models of the motor ship SAN FRANCISCO were tested. Although within the limits of the investigation there were no differences in the behavior of the models that could be ascribed to the effect of scale, several very noticeable effects were found that resulted from the dynamics of the towing system employed.

1. Ship models--Seaworthiness --Scale effects
2. Ship models--Motion-- Testing equipment
3. Ship models--Model TMB 3572-5A
4. Ship models--Model TMB 3572-8
5. SAN FRANCISCO (German Cargo ship)
I. Reiss, Howard R.

David Taylor Model Basin. Report 1039.
THE EFFECTS OF SCALE AND TOWING SYSTEM ON WAVE TESTS OF SMALL SHIP MODELS, by Howard R. Reiss. May 1961. v, 41p. illus., photos., graphs, refs. UNCLASSIFIED

To investigate experimentally the effect of scale on the motions of ship models in waves, two different scale models of the motor ship SAN FRANCISCO were tested. Although within the limits of the investigation there were no differences in the behavior of the models that could be ascribed to the effect of scale, several very noticeable effects were found that resulted from the dynamics of the towing system employed.

1. Ship models--Seaworthiness --Scale effects
2. Ship models--Motion-- Testing equipment
3. Ship models--Model TMB 3572-5A
4. Ship models--Model TMB 3572-8
5. SAN FRANCISCO (German Cargo ship)

I. Reiss, Howard R.

David Taylor Model Basin. Report 1039.
THE EFFECTS OF SCALE AND TOWING SYSTEM ON WAVE TESTS OF SMALL SHIP MODELS, by Howard R. Reiss. May 1961. v, 41p. illus., photos., graphs, refs. UNCLASSIFIED

To investigate experimentally the effect of scale on the motions of ship models in waves, two different scale models of the motor ship SAN FRANCISCO were tested. Although within the limits of the investigation there were no differences in the behavior of the models that could be ascribed to the effect of scale, several very noticeable effects were found that resulted from the dynamics of the towing system employed.

1. Ship models--Seaworthiness --Scale effects
2. Ship models--Motion-- Testing equipment
3. Ship models--Model TMB 3572-5A
4. Ship models--Model TMB 3572-8
5. SAN FRANCISCO (German Cargo ship)

I. Reiss, Howard R.

David Taylor Model Basin. Report 1039.
THE EFFECTS OF SCALE AND TOWING SYSTEM ON WAVE TESTS OF SMALL SHIP MODELS, by Howard R. Reiss. May 1961. v, 41p. illus., photos., graphs, refs. UNCLASSIFIED

To investigate experimentally the effect of scale on the motions of ship models in waves, two different scale models of the motor ship SAN FRANCISCO were tested. Although within the limits of the investigation there were no differences in the behavior of the models that could be ascribed to the effect of scale, several very noticeable effects were found that resulted from the dynamics of the towing system employed.

1. Ship models--Seaworthiness --Scale effects
2. Ship models--Motion-- Testing equipment
3. Ship models--Model TMB 3572-5A
4. Ship models--Model TMB 3572-8
5. SAN FRANCISCO (German Cargo ship)

I. Reiss, Howard R.

David Taylor Model Basin. Report 1039.
THE EFFECTS OF SCALE AND TOWING SYSTEM ON WAVE TESTS OF SMALL SHIP MODELS, by Howard R. Reiss. May 1961. v, 41p. illus., photos., graphs, refs. UNCLASSIFIED

To investigate experimentally the effect of scale on the motions of ship models in waves, two different scale models of the motor ship SAN FRANCISCO were tested. Although within the limits of the investigation there were no differences in the behavior of the models that could be ascribed to the effect of scale, several very noticeable effects were found that resulted from the dynamics of the towing system employed.

1. Ship models--Seaworthiness --Scale effects
2. Ship models--Motion-- Testing equipment
3. Ship models--Model TMB 3572-5A
4. Ship models--Model TMB 3572-8
5. SAN FRANCISCO (German Cargo ship)

I. Reiss, Howard R.